Gastro Hep Advances 2024;3:551–561

ORIGINAL RESEARCH—BASIC

CA19-9-Positive Extracellular Vesicle Is a Risk Factor for Cancer-Associated Thrombosis in Pancreatic Cancer

Chikako Shibata, Motoyuki Otsuka, Kazunaga Ishigaki, Takahiro Seimiya, Takahiro Kishikawa, and Mitsuhiro Fujishiro

Department of Gastroenterology, Graduate School of Medicine, The University of Tokyo, Tokyo, Japan

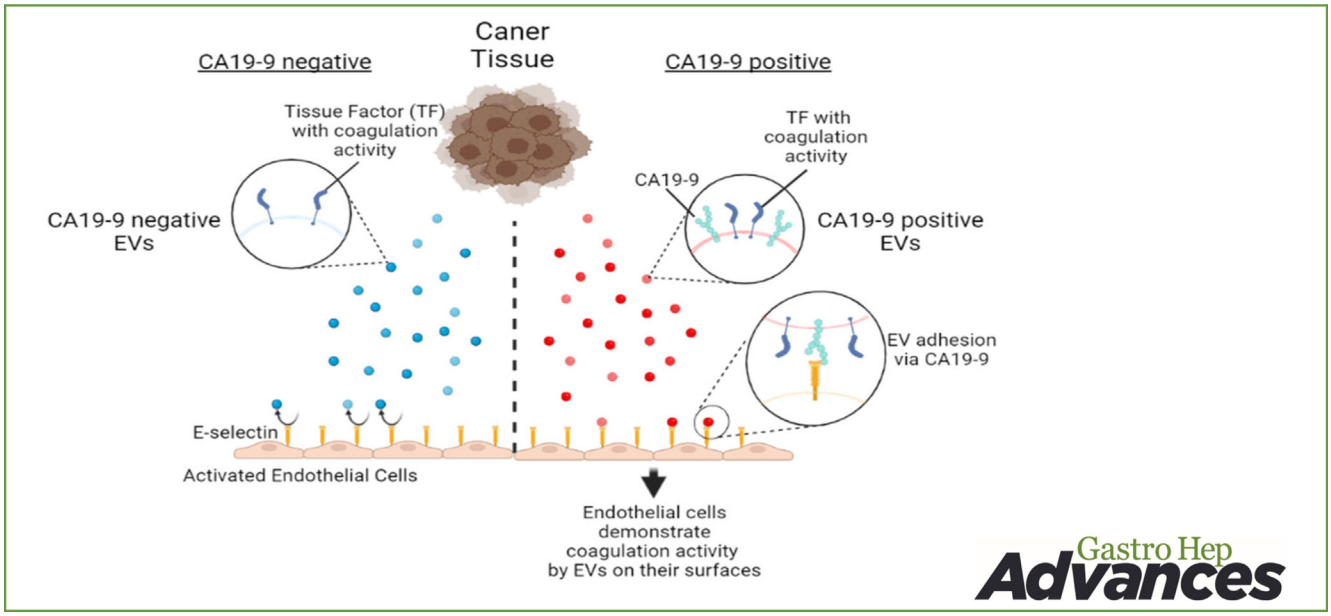

BACKGROUND AND AIMS: Cancer-associated venous thromboembolism (VTE) is a frequent complication associated with high mortality in patients with cancer, particularly pancreatic cancer. While biological factors such as coagulation factors released from cancer cells may underlie the mechanisms of cancer-associated VTE, the detailed mechanisms have not been determined. Here, we aimed to determine whether extracellular vesicles carrying a glycan sialyl-Lewis[a], known as carbohydrate antigen 19-9 (CA19-9), which is a clinically used serum tumor marker and selectin ligand, are a significant cause of cancer-associated VTE. **METHODS:** Risk factors for cancer-associated VTE were determined using clinical data. EVs derived from CA19-9-deficient or overexpressing pancreatic cancer cells were characterized. The protein levels of coagulation factors on the surface of the EVs were quantified using our newly developed sensitive method. **RESULTS:** Higher CA19-9 levels in the sera of patients were significantly associated with the occurrence of VTE. Using CA19-9-negative or overexpressing pancreatic cancer cells, we found that EVs derived from these cells interacted with E-selectin of endothelial cells in a CA19-9-dependent manner in cell-based assays and in vitro blood vessel models. EVs derived from cancer cells have higher tissue factor levels on their surfaces, and increased tissue factor activity is induced locally, where CA19-9-positive EVs bind to activated endothelial cells. **CONCLUSION:** These results suggest that the binding between CA19-9-positive EVs released from cancer cells and endothelial cell E-selectin explains the increased frequency of VTE in patients with pancreatic cancer.

Keywords: E-selectin; Glycan; Tissue Factor; Coagulation; Endothelial Cell

Introduction

Cancer-associated venous thromboembolism (VTE) is closely associated with mortality in patients with cancer.[1] It is the second-largest cause of death, followed by deaths due to cancer progression. Thromboembolic events such as pulmonary embolism directly or indirectly lead to death in patients with cancer.[2] Particularly in patients with pancreatic cancer, the incidence of VTE is 8.1%, which is the highest among various types of cancer.[1]

Thrombi may form in patients with cancer due to Virchow's triad as well as their clinical background, such as

Abbreviations used in this paper: **CA19-9, carbohydrate antigen 19-9; EVs, extracellular vesicles; HUVEC, human umbilical vein endothelial cell; SELE, E-selectin; VTE, venous thromboembolism.**

Most current article

2772-5723
https://doi.org/10.1016/j.gastha.2024.02.005

cancer stage, comorbidities, low-performance status, and postoperative state. Virchow's triad refers to venous stasis, hypercoagulability, and endothelial injury. These states can be caused by direct pressure or tumor invasion, and by various tumor-secreted fluid factors.[3] Several studies have suggested that biologically active substances released from cancer cells, such as tissue factor (TF), plasminogen activator inhibitor-1, cysteine protease, inflammatory cytokines, and platelet aggregation agonists, can cause cancer-associated VTE. However, the detailed mechanisms underlying this process have not yet been elucidated.

Extracellular vesicles (EVs) are secreted nanoparticles from cells that carry various biological molecules such as nucleic acids, proteins, lipids, and glycans. They play pivotal roles in intercellular communication in both healthy and pathological conditions. EVs affect the surrounding cells and can enter blood vessels to affect distant organs. EVs have been shown to be involved in cancer-related pathogenesis.[4] TFs, the initiators of the extrinsic pathway of coagulation,[5] exist in some cancer cell-derived EVs,[6–8] and such EVs may induce coagulation.

Proteins and glycans on the surfaces of EVs are biologically important because these surface antigens determine the specific recipient cells of EVs and exert biological effects by interacting with extracellular molecules on recipient cell surfaces.[4]

Carbohydrate antigen (CA) 19-9 is a commonly used tumor marker in patients with cancer, especially pancreatic cancer. Interestingly, some studies suggest that high serum CA19-9 levels are associated with thrombosis. For example, the presence of both CA19-9-positive cancer tissues and higher CA19-9 levels in the sera of patients with cancer are significantly associated with abnormal coagulation in gastric cancer.[9] Higher serum CA19-9 levels are associated with an increased generation of thrombin in the plasma.[10] Furthermore, given the process of EV generation, the glycoprotein CA19-9 is expected to exist on their surface. Together with the fact that the incidence of thrombosis in patients with pancreatic cancer is the highest among cancers, we hypothesized that CA19-9-positive EVs released from pancreatic cancer cells tend to adhere more to endothelial cells, resulting in local thrombosis by the TFs on EVs because CA19-9 is a lectin ligand of E-selectin (SELE), which is highly expressed on the surface of activated endothelial cells.

In this study, we aimed to determine the factors associated with the risk of cancer-associated VTE and the underlying mechanisms; for this reason, we examined the coagulation activity of human endothelial cells treated with CA19-9-positive and negative EVs in in vitro vessel models and analyzed the clinical data of patients with pancreatic cancer, with or without thrombosis.

Methods

Cell Culture

BxPC-3 and Capan-2 cells, CA19-9-positive human pancreatic cancer cell lines, and 293T cells were purchased from the American Type Culture Collection (ATCC Manassas, VA, USA). PANC-1 cells and CA19-9-negative human pancreatic cancer cell line were purchased from the European Collection of Authenticated Cell Cultures (ECACC, Wiltshire, UK). Human umbilical vein endothelial cells (HUVECs), immortalized by hTERT, were purchased from the Japanese Collection of Research Bioresources (Osaka, Japan). Details of the culture condition are described in Supplementary Methods.

Isolation of EVs

EVs were isolated using the ultracentrifuge. Details are in Supplementary Methods.

Deletion of CA19-9 in BxPC-3 and Capan-2 Cells

CA19-9-deleted cells were established by disrupting the FUT3 gene, which encodes a glycosyltransferase essential in the final process of synthesizing the sugar chain CA19-9. To disrupt *FUT3*, lentiCRISPR v2 (Plasmid #52961, Addgene, Watertown, MA, USA), which constitutively expresses the Cas9 protein and a guide RNA, was used as previously reported.[11] Details are in Supplementary Methods.

Overexpression of CA19-9 in PANC-1 Cells

A series of glycosyltransferases is essential for the production of CA19-9. Referring to the previous report,[12] 2 glycosyltransferases essential for CA19-9 production, β3GALT5 and FUT3 were simultaneously overexpressed in PANC-1 cells. The β3GALT5-coding sequences were amplified by polymerase chain reaction (PCR) using BxPC-3 cDNA as templates, and the FUT3-coding sequences were amplified by PCR using the pF1KE6892 as templates (Kazusa DNA Research Institute, Chiba, Japan). Plasmids carrying *FUT3* and *β3GALT5* were cloned into the pCDH vector (System Biosciences) to produce lentiviruses. PANC-1 cells were incubated with these lentiviruses for 2 days, followed by selection using 2 μg/ml puromycin for 7 days. Successful overexpression of CA19-9 was confirmed using western blotting.

Activation of Endogenous SELE Transcription in HUVECs

HUVECs were treated with 10 ng/ml of human tumor necrosis factor-α (TNFα) (Wako) for 12 h to induce SELE expression.[13] SELE-overexpressing HUVECs (HUVEC-SELE) were established using the CRISPR-a-expressing lentiviruses, which activate the endogenous SELE transcription (E-selectin Lentiviral Activation Particles, sc-400452-LAC; Santa Cruz Biotechnology, Dallas, TX), according to the manufacturer's instructions. Briefly, viral particles were added to the cells and incubated for 2 days. Subsequently, the cells were selected using 1 μg/ml of puromycin, 5 μg/ml of blasticidin, and 5 μg/ml of hygromycin for 2 days. SELE overexpression was confirmed using western blotting analysis.

SELE Expression on the Cell Surface

Flow cytometry analysis was performed to confirm SELE overexpression on the surface of HUVECs. Details are in Supplementary Methods. Fluorescence intensities were determined using a Guava EasyCyte Plus Flow Cytometry System (Guava Technologies, Hayward, CA, USA), as described previously.[14]

Adhesion Analysis of EVs by Flow Cytometry

EVs (approximately 1.0×10^{10} particles) were fluorescently labeled with the ExoSparkler Exosome Membrane Labeling Kit-Green (Dojido) according to the manufacturer's instructions. The labeled EVs and HUVEC-SELE cells were mixed and rotated for 30 minutes at room temperature. After incubation, the fluorescence intensities, which reflect the levels of EVs attached to the cell surface, were analyzed using a Guava EasyCyte Plus Flow Cytometry System.

Confirmation of the Existence of CA19-9 on the Surfaces of EVs

After 1 μg of CA19-9 antibody (010-25901, Wako) and 0.5 μl of Alexa Fluor Plus 405 (#A48255, Thermo Fisher Scientific, Waltham, MA, USA) were mixed at room temperature for 1 hour, BxPC-3 Pos cell-derived EVs (approximately 1.0×10^{10} particles) were added and fluorescently labeled at 4 °C overnight. Isotypic IgG was used as a negative control. Labeled EVs were analyzed the next day using CytoFLEX (Beckman Coulter, Brea, CA, USA) with a violet laser.

Electron Microscopy

Scanning electron microscopy using the NanoSuit method, which enables observation of samples under wet conditions, was conducted at NanoSuit Inc. (Shizuoka, Japan) to visualize the adhesion of EVs derived from BxPC-3 and HUVEC-SELE cells. After the cells were incubated with EVs at 37 °C for 4 hours, they were treated with 2% NanoSuit Solution Type III, followed by observation using the Field Emission Scanning Electron Microscope (JEM-7100F, JEOL; S-4800, Hitachi, Tokyo, Japan).

Surface Plasmon Resonance

Surface plasmon resonance analysis was conducted at the Toray Research Center (Tokyo, Japan). The SELE recombinant protein (R&D Systems, Minneapolis, MN, USA) was fixed onto the sensor chip, and CA19-9-positive or negative EVs were injected into the surface plasmon resonance device.

Adhesion Analysis of EVs in the In Vitro Blood Vessel Model

An in vitro blood vessel model on a microscope slide was prepared by CSTEC Corporation (Kyoto, Japan). The glass slide was covered with laser-processed double-sided tape and a cycloolefin polymer film. The width of the laser-processed channel was 500 μm and the depth was 300 μm, and both ends of the channel were perforated on the outside. To cover the inside of the channel with HUVECs, 200 ng/ml of human fibronectin (Wako) was poured into the channels from one end, and the slides were incubated at 4 °C overnight. The next day, after washing the channels with phosphate buffered saline (PBS), HUVEC-SELE cells were seeded into the channel and incubated at 37 °C overnight. EVs (approximately 1.0×10^{10} particles) labeled with the ExoSparkler Exosome Membrane Labeling Kit-Green (Dojido) were poured into the channel. After incubation at 37 °C for 15 h, the vessels were observed using the Olympus DP72 microscope digital camera system with DP2-TWAIN software (Olympus, Tokyo, Japan).

Flow Cytometry Analysis of Beads-Bound EVs

To detect TF on the surface of EVs, flow cytometry analysis was performed using the PS Capture Exosome Flow Cytometry Kit (Wako). Details are in Supplementary Methods.

TF Activity Assay

The TF activities of EVs and HUVEC-SELE cell lysates were analyzed using the Human Tissue Factor Chromogenic Activity Kit (Assay Pro, St. Charles, MO, USA). Details are in Supplementary Methods.

Detection of the Proteins of Interest on the Surface of EVs by the "Tag Method"

To detect and quantitate the proteins of interest on the surface of EVs conveniently, a new "tag method" was established using the antibodies conjugated with specific oligonucleotides. Pierce Protein A/G Magnetic Beads (3 μL, Thermo Fisher Scientific) and capture antibodies (4.5 μg) were mixed at room temperature for 1 hour. The beads were washed with immunoprecipitation buffer (50 mM Tris [pH 7.5], 150 mM NaCl, 0.1% NP40, 1 mM ethylenediaminetetraacetic acid [pH 8.0], 0.25% gelatin, and 0.02% sodium azide). Normal mouse IgG (140-09511, Wako) was added and mixed at room temperature for 1 hour to prevent nonspecific binding of the detection antibodies to the beads. After washing, 10% bovine serum albumin (Wako) in PBS was added and mixed at room temperature for 1 hour to prevent nonspecific protein binding. EVs (approximately 1.5×10^{10} particles) in PBS were added to the beads and mixed by rotation at 4 °C overnight. The beads were washed with immunoprecipitation buffer, and then detection antibodies conjugated with antibody-specific oligonucleotides were added (1:100,000 dilution in PBS) and mixed with rotation at 4 °C overnight. Detection antibodies conjugated with specific oligonucleotides and sold as TotalSeq antibodies were purchased from commercial sources. After the beads were washed, deionized distilled water (7 μL) was added to beads, and beads were boiled at 95 °C for 10 min. Specific oligonucleotides, nucleic acids, and other EV components were detached from the beads into the supernatant. Specific oligonucleotides in the supernatants (1 μL) were quantified by qPCR. The primers were designed according to common regions at both ends of the oligonucleotide. The sequences were as follows: forward 5'-GTGACTGGAGTTCAGACGTG-3' and reverse 5'-TTGCTAGGACCGGCCTTA-3'. To confirm that the EVs were successfully captured on the beads using capture antibodies, western blotting analyses were performed using beads with captured EVs. The beads were incubated with the sampling buffer on ice for 15 minutes. For the input lane, approximately 7.5×10^8 particles of EVs were added. To confirm that specific sequences were amplified by qPCR, TA cloning of the amplified PCR products was performed using a TOPO TA Cloning Kit (Thermo Fisher Scientific), followed by Sanger sequencing at Eurofins Genomics (Tokyo, Japan). The capture antibodies used were as follows: CD63 (012-27063), CD9 (014-27763), and CA19-9 (010-25901) antibodies (Wako). The following detection antibodies were used: TotalSeq-B0404, anti-human CD63 (353049); TotalSeq-B0579, anti-human CD9 (312123); and TotalSeq-B0822, anti-human CD142 (TF) (365209) (BioLegend).

RNA Sequencing

RNA sequencing data were acquired at Rhelixa (Tokyo, Japan). Details are in Supplementary Methods. The raw data are available with GEO accession: GSE227567.

Clinical Data and Serum Samples

Clinical data were obtained from 432 patients diagnosed with pancreatic cancer at the University of Tokyo Hospital from April 2001 to July 2015. The diagnosis of thrombosis was made based on clinical symptoms and confirmed using contrast-enhanced computed tomography or ultrasound scanning. Serum samples were collected from patients diagnosed with pancreatic cancer at the University of Tokyo Hospital from January 2022 to December 2022. Written informed consent was obtained from all patients whose sera were used. The study protocol was approved by the Ethics Committee of the University of Tokyo Hospital (No. 11712).

Immunohistochemistry, Immunofluorescence, Western Blotting Analysis, and RT-qPCR

Details are in Supplementary Methods.

Statistical Analysis

Statistical analyses and data visualization were performed using the R statistical software. *P*-values were determined by unpaired two-tailed *t*-tests; $P < .05$ was considered to indicate statistical significance. A logistic regression model was used to calculate the odds ratio with 95% confidence interval for the risk of thrombosis associated with CA19-9 levels and other potential confounding factors.

Results

Higher Levels of CA19-9 in the Sera are Clinically a Significant Risk Factor for Cancer-Associated VTE

To determine the risk factors for cancer-associated thrombosis during the course of pancreatic cancer, the clinical data of 432 patients were analyzed (Table 1). Among them, 50 patients developed vein thrombosis during the course of the disease. The logistic regression model showed that higher levels of CA19-9 in the sera were significantly associated with the risk of thrombosis, with odds ratio of 2.31 (95% confidence intervals: 1.17–4.43, $P = .013$) (Table 2 and Figure 1). No other factors including age, cancer stage, performance status (PS), or body mass index were significantly associated with the risk of thrombosis (Figure 1).

Establishment of CA19-9-Nonexpressing or Overexpressing EVs Derived From Pancreatic Cancer Cells

CA19-9 is present in the EVs released from CA19-9-positive pancreatic cancer cells.[11] To examine the biological role of CA19-9 in thrombosis, CA19-9-positive and negative EVs were isolated from CA19-9-positive and negative pancreatic cancer cell lines, respectively. Additionally, we established CA19-9-nonexpressing cells from CA19-9-positive pancreatic cancer cell lines and CA19-9-overexpressing cells from CA19-9-negative pancreatic cancer cell lines to isolate CA19-9-positive or negative EVs, respectively, from these isogenic cells.

A series of glycosyltransferases are essential for the synthesis of CA19-9[15] (Figure 2A). While the BxPC-3 and Capan-2 cell lines normally produce CA19-9, the expression of CA19-9 is inhibited by disrupting the fucosyltransferase 3 (FUT3) gene, a glycosyltransferase required for the synthesis of CA19-9. Inhibition of CA19-9 expression was confirmed using wild-type cells (CA19-9-positive) and FUT3 gene-disrupted cells (CA19-9-negative) by western blotting analysis (Figure 2B, left and middle panel). In contrast, while CA19-9 is normally not produced in pancreatic cancer cell line PANC-1 cells, the expression of CA19-9 was induced by the forced expression of 2 glycosyltransferases, galactosyltransferase (β3GALT5) and FUT3. Overexpression of CA19-9 was confirmed in wild-type (CA19-9-negative) and glycosyltransferase-overexpressing cells (CA19-9-positive) (Figure 2B, right panel). In addition, the expression of CA19-9 in the EVs derived from each cell line was confirmed by western blotting analysis, which showed that the expression of CA19-9 in the EVs was consistent with the expression of CA19-9 in each cell line (Figure 2C).

No significant differences were observed in the size distribution of the isolated EVs or in the images of the EVs, irrespective of CA19-9 expression (Figure 2D and E). Universal EV markers, CD63 and flotillin 2 (FLOT2), were expressed in both cell lysates and EVs, whereas calnexin, an endoplasmic reticulum marker, was not expressed in the EVs (Figure 2F). The CD63 band size differed between cell types, which is consistent with previous reports.[16,17] These results confirmed that the EVs were appropriately isolated. Furthermore, flow cytometry analyses showed that CA19-9 was expressed on the surface of EVs (Figure 2G).

CA19-9-Positive EVs Tend to Adhere to SELE-Expressing Endothelial Cells

Since CA19-9 is a lectin ligand that readily binds to E-selectin, we examined whether there were any differences in the adhesion levels of CA19-9-positive and negative EVs from pancreatic cancer cells and SELE-expressing endothelial cells. While TNFα upregulates SELE expression levels on vascular endothelial cells (Figure A1A) and high TNFα levels are observed in the sera of patients with pancreatic cancer,[18] we here established SELE-overexpressing HUVEC lines (HUVEC-SELE) (Figure A1A and B) to mimic endothelial cells in patients with pancreatic cancer, with avoidance of the other effects of TNFα.

Flow cytometry analyses after adding CA19-9-positive or negative EVs to HUVEC-SELE cells showed that a higher number of CA19-9-positive EVs adhered to the cells than CA19-9-negative EVs did (Figure 3A). Indeed, CA19-9-positive EVs from BxPC-3 cells were attached to the surface of HUVEC-SELE (Figure 3B), as observed by electron microscopy using the NanoSuit method.[19] Surface plasmon resonance analysis

Table 1. Clinical Features of the Participants at Baseline

Parameters	Total N = 432	With thrombus n = 50	Without thrombus n = 382	*P*-value
CA19-9				
<5000 U/ml	349	34 (68.0%)	315 (82.5%)	.015
≥5000 U/ml	83	16 (32.0%)	67 (17.5%)	
Age				
<65 years	166	16 (32.0%)	150 (39.3%)	.32
≥65 years	266	34 (68.0%)	232 (60.7%)	
Stage (UICC)				
IA or IB	5	0 (0.0%)	5 (1.3%)	.65
IIA or IIB	39	5 (10.0%)	34 (8.9%)	
III	119	11 (22.0%)	108 (28.3%)	
IV	269	34 (68.0%)	235 (61.5%)	
PS				
0–1	407	47 (94.0%)	360 (94.2%)	.95
2–4	25	3 (6.0%)	22 (5.8%)	
BMI				
<22	264	31 (62.0%)	233 (61.0%)	.89
≥22	168	19 (38.0%)	149 (39.0%)	

Stage: Cancer stages based on the TNM Classification defined by UICC.
BMI, body mass index; PS, performance status; UICC, Union for International Cancer Control.

revealed that CA19-9-positive EVs adhered to the recombinant SELE protein on the sensor chip in a concentration-dependent manner. However, CA19-9-negative EVs rarely adhered to SELE (Figure 3C). Furthermore, in vitro vessel models showed that CA19-9-positive EVs derived from wild-type BxPC-3 cells more readily adhered to HUVEC-SELE compared to CA19-9-negative EVs from FUT3 gene-disrupted BxPC-3 cells (Figure 3D). These results suggested that CA19-9-positive EVs released from pancreatic cancer cells tended to adhere to SELE-expressing endothelial cells.

Establishment of a "Tag Method" to Quantitate the Protein Levels on the Surface of EVs

Because CA19-9 is a clinical risk factor for VTE in pancreatic cancer, we wanted to determine if coagulation factors exist on the surface of EVs that adhere to endothelial cells. However, it is challenging to examine and quantify protein levels on the surface of EVs because their size is too small for analysis by conventional flow cytometry. To overcome these limitations, we established a new "tag method" to examine the protein levels on the surface of EVs correctly and conveniently. First, EVs were captured on beads using known surface markers such as CD63 or CD9. Next, antibodies against the proteins of interest, conjugated with specific oligonucleotide "tags," were added to the EV-bead complexes. After washing the complexes, the oligonucleotide tags were collected and subjected to qPCR to quantify the oligonucleotides, which reflect the levels of the protein of interest on the surface of the EVs (Figure A2A).

To confirm the rigidity of this method, we captured EVs on beads with a CD63 antibody (Figure A2B), and the well-known surface proteins CD9 and CD63 on EVs were quantified using corresponding antibodies conjugated with

Table 2. Logistic Regression Analysis on Factors Associated With Thrombosis

Variable	OR (95% CI)	*P*-value
CA19-9 ≥ 5000 U/ml	2.31 (1.17, 4.43)	.013
Age ≥ 65 y	1.44 (0.77, 2.80)	.26
Stage (UICC) III or IV	0.94 (0.37, 2.86)	.90
PS ≥ 2	0.92 (0.21, 2.86)	.90
BMI ≥ 22	0.94 (0.50, 1.73)	.83

BMI, body mass index; CI, confidence interval; OR, odds ratio; PS, performance status; UICC, Union for International Cancer Control.

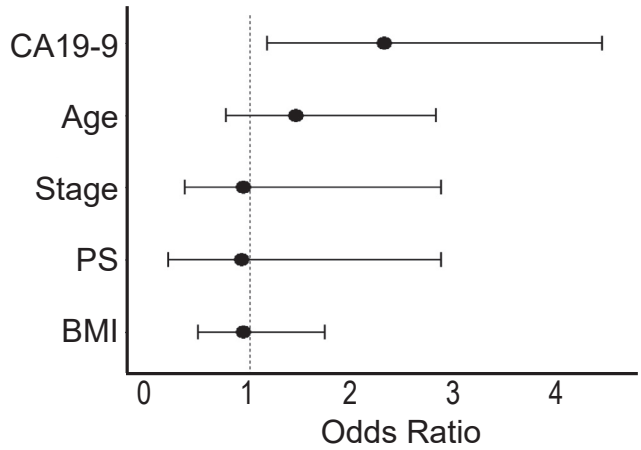

Figure 1. Risk of thrombosis in patients with pancreatic cancer. The logistic regression model revealed that high CA19-9 levels were associated with the risk of thrombosis. Clinical data at diagnosis were obtained from patients with pancreatic cancer (n = 432). Thrombosis occurred in 50 patients during the course of this study. The average observation time until thrombosis or death was 382 days.

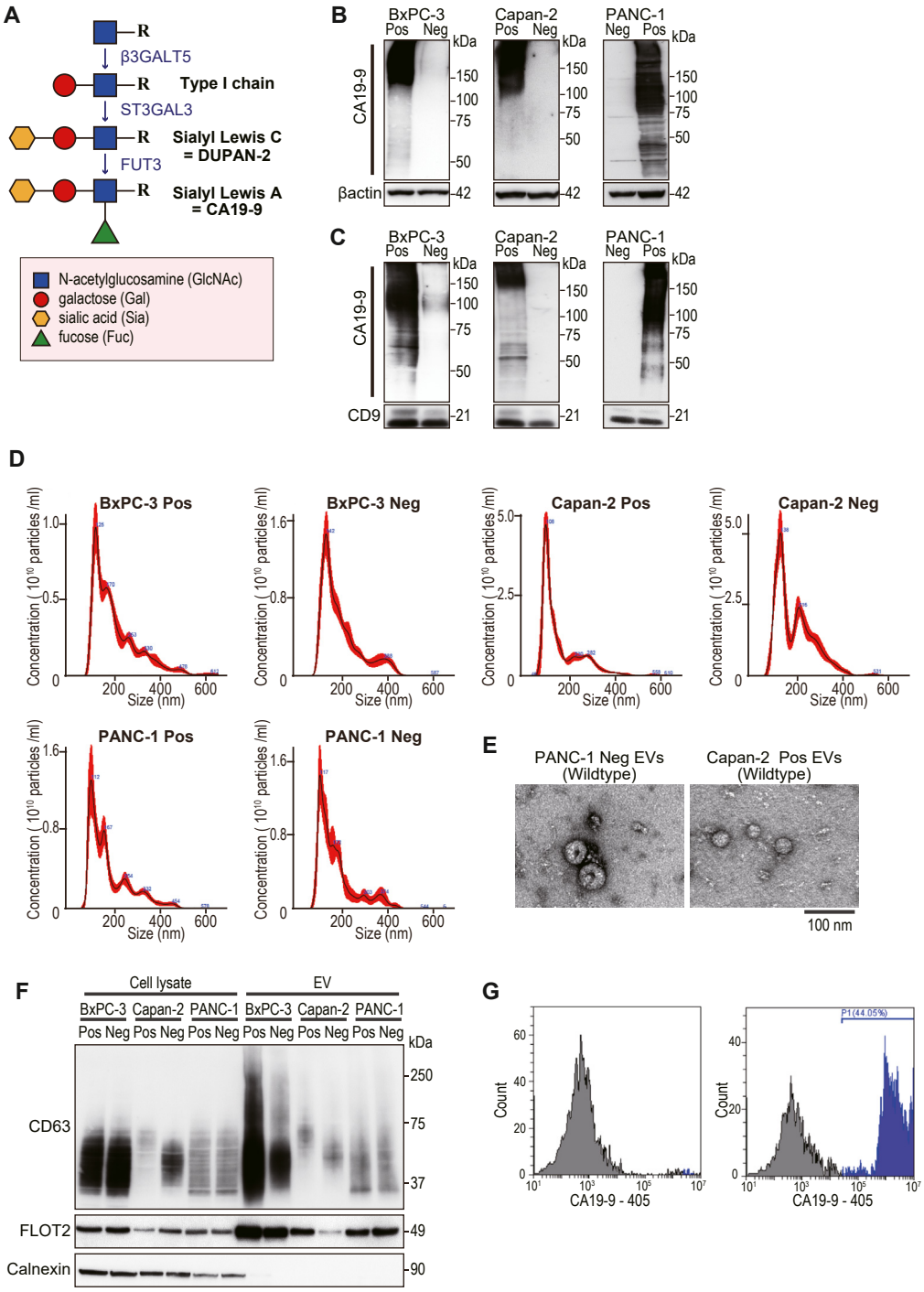

Figure 2. Establishment of CA19-9-nonexpressing or overexpressing cell lines. (A) Illustration of the synthesis of CA19-9. A series of glycosyltransferases, such as β3GALT5 and FUT3, are crucial for the synthesis of CA19-9. (B) Establishment of CA19-9-nonexpressing (CA19-9-negative: Neg) cell lines from BxPC-3 and Capan-2 cells by disrupting *FUT3* expression using the CRISPR-Cas9 system (left and middle panels). Establishment of CA19-9-overexpressing cell line (CA19-9-positive: Pos) from PANC-1 cells, which are originally CA19-9-nonproducing, by overexpression of glycosyltransferases β3GALT5 and FUT3 (right panel). Representative images from 3 independent western blotting experiments with the indicated cell lysates are shown. (C) Representative images of 3 independent western blotting experiments examining the expression of CA19-9 in EVs derived from the indicated cell lines. Representative images from 3 independent western blotting experiments are shown. The molecular size of CA19-9 varies between cells due to differences in glycosylation. (D) Size distribution of EVs derived from the indicated cell culture media. (E) Representative transmission electron microscopy images of EVs derived from the cell culture media of PANC-1 Neg and Capan-2 Pos cells. Scale bar: 100 nm. (F) Western blotting analyses of EV markers (CD63 and FLOT2) and an endoplasmic reticulum marker (calnexin). Cell lysates (2.8 μg) and lysates of EVs (approximately 1.0×10^{10} particles) isolated from the cell culture media were applied. Representative images from 3 independent experiments are shown. The molecular size of CD63 varies between cells due to differences in glycosylation. (G) Flow cytometry analyses show that EVs derived from BxPC-3 Pos cells had CA19-9 on their surface. The right figure indicates that CA19-9 was present on the surface of 44% of these EVs. The left figure shows the negative control, with isotypic IgG.

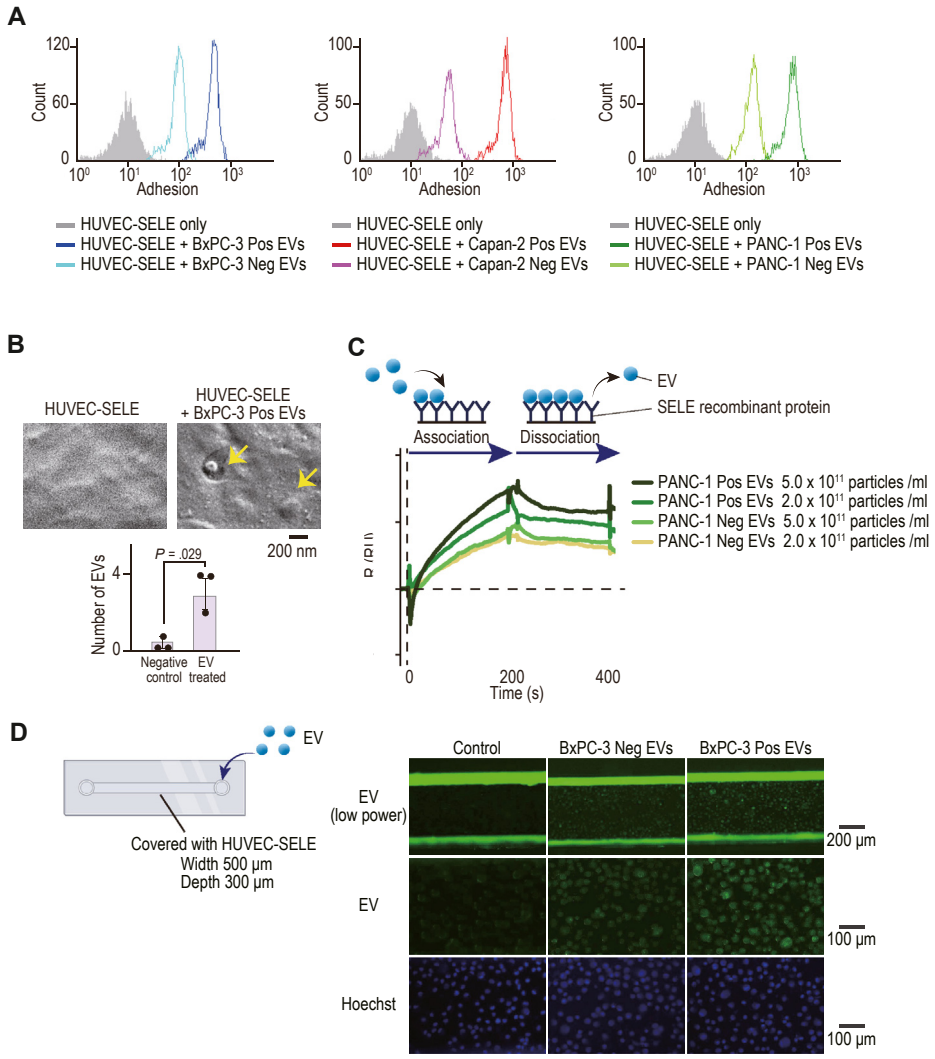

Figure 3. Adhesion of CA19-9-positive EVs to E-selectin. (A) Adhesion levels of CA19-9-positive (Pos) or negative (Neg) EVs derived from 3 cell lines to HUVEC-SELE (HUVECs overexpressing E-selectin) were determined by flow cytometry. CA19-9-positive EVs attached more to HUVEC-SELE cells than CA19-9-negative EVs. Representative histograms of 3 independent experiments are shown. (B) Representative scanning electron microscopy images using the nanosuit method. HUVEC-SELE cells were treated with CA19-9-positive EVs from BxPC-3 cells (BxPC-3 Pos) for 4 h. Arrows indicate BxPC-3 EVs infiltrating the HUVEC-SELE. Scale bar: 200 nm. (Below) Quantification of the number of the possible exogenous EVs observed in each field. The number of EVs were counted in 3 fields of HUVEC-SELE cells (negative control) and HUVEC-SELE cells treated with EVs (EVs treated). Data are means ± SD. *P*-values are shown in figure. (C) Interaction between recombinant human SELE protein and CA19-9-positive or negative EVs (Panc-1 Pos EVs or Neg EVs) as determined by surface plasmon resonance. CA19-9-positive EVs attached in a dose-dependent manner and were difficult to detach. (D) Representative images of EV adhesion to HUVEC-SELE in an in vitro blood vessel model. CA19-9-positive or negative EVs from BxPC-3 cells (BxPC-3 Pos EVs or BxPC-3 Neg EVs) stained with green dye were poured into a blood vessel model covered with HUVEC-SELE cells. The nuclei of HUVECs were stained with Hoechst (blue). Scale bar: 100 μm (upper row) or 200 μm (middle and lower row). Autofluorescence showing the 2 green lines (upper row) indicates the vessel walls.

specific oligonucleotide tags (Figure A2C and D). Similarly, EVs were captured on beads using CD9 or CA19-9 antibodies, and we confirmed that CD9 or CD63 proteins on EVs were successfully detected using this method (Figure A2E and F). These results suggest that the method applied here using oligonucleotide tags is a powerful tool for quantifying protein levels on the surface of EVs.

TFs Exist on the Surface of EVs, Which Are Derived From Pancreatic Cancer Cells

To determine the molecular mechanisms by which higher levels of CA19-9 in sera result in increased thrombosis, we hypothesized that CA19-9-positive EVs adhere more to endothelial cells with SELE, followed by thrombosis due to coagulation factors on the EVs. Among the

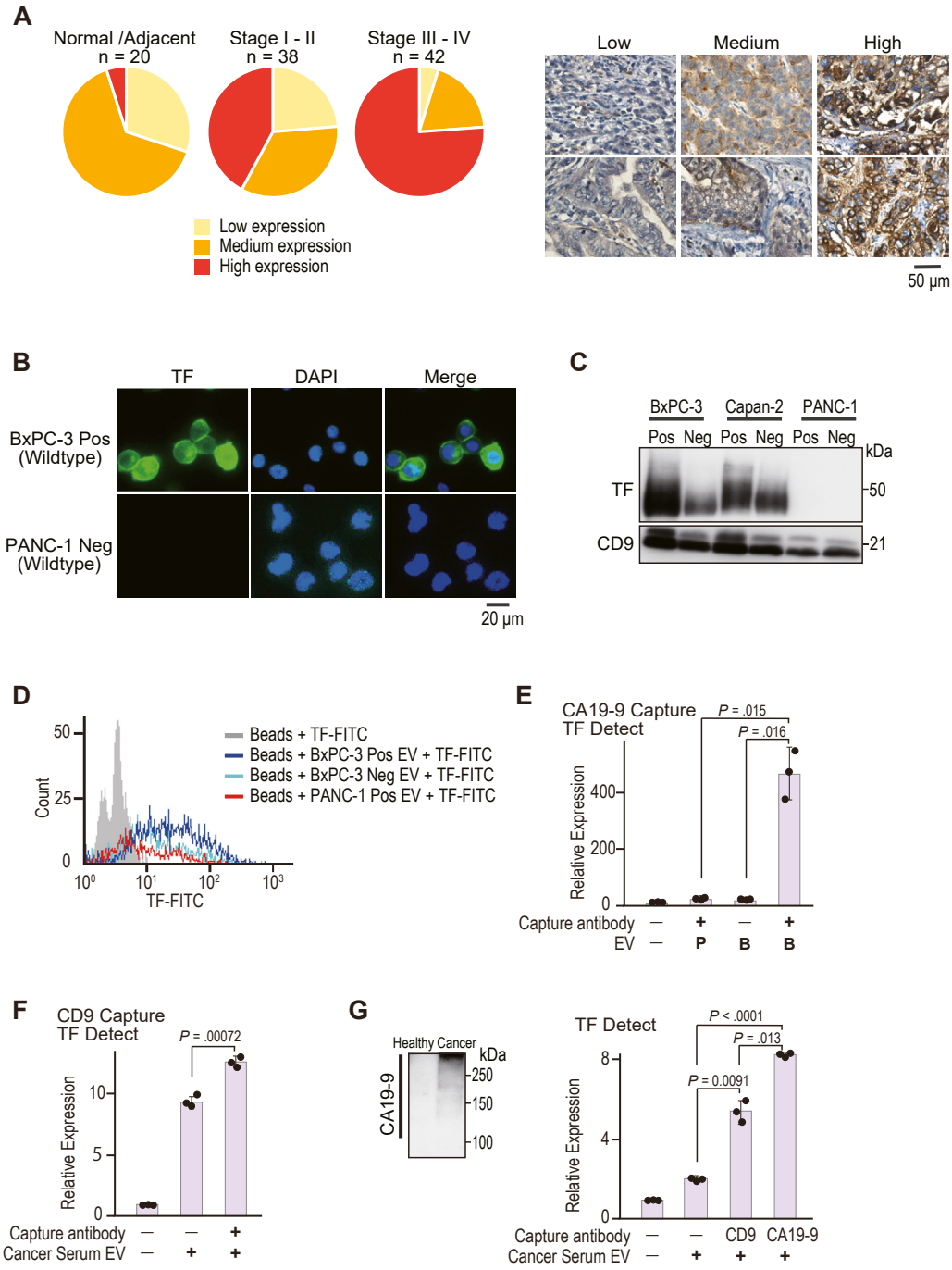

Figure 4. Tissue factors (TFs) were expressed at the surface of pancreatic cancer cell-derived EVs. (A) High TF expression levels especially in advanced pancreatic cancer tissues were detected by immunohistochemistry using anti-TF antibody. Representative images of low, medium, and high TF expression levels are shown on the right side. Scale bar: 50 μm. (B) Immunofluorescent images of TFs (green) in BxPC-3 and PANC-1 cells. The nuclei were stained with 4',6-diamidino-2-phenylindole (DAPI) (blue). Representative images from 3 independent experiments are shown. Scale bar: 20 μm. (C) Western blotting analyses of TFs in the lysate of the indicated EVs (approximately 1.0×10^{10} particles). Representative images from 3 independent western blotting experiments are shown. (D) TF expression levels on the surface of EVs, as determined by flow cytometry. TFs on the surface of EVs were stained with fluorescein isothiocyanate (FITC) after capturing the indicated EVs on the beads for flow cytometry. Representative histograms of 3 independent experiments are shown. (E) TF expression levels on the surface of PANC-1CA19-9-positive EVs (P) and BxPC-3 CA19-9-positive EVs (B) as determined by qPCR using the tag method. Data are means ± SD ($n = 3$). *P*-values are shown in figure. (F) TF expression levels in the pooled cancer patient serum-derived EVs determined by the tag method after the capture of EVs using CD9 antibody. Data are means ± SD ($n = 3$). *P*-values are shown in figure. (G) Western blotting analyses of CA19-9 in the lysate of the pooled healthy donor serum-derived EVs and pooled cancer patient serum-derived EVs (1.0×10^{10} particles). TF expression levels in cancer patient serum-derived EVs after the capture of EVs by CD9 and CA19-9 antibodies. EVs captured by the CA19-9 antibody, namely CA19-9-positive EVs, had significantly more TFs on their surfaces. Data are means ± SD ($n = 3$). *P*-values are shown in figure. All statistical analyses were performed using the Welch's *t*-tests. Neg, CA19-9-negative; Pos, CA19-9-positive.

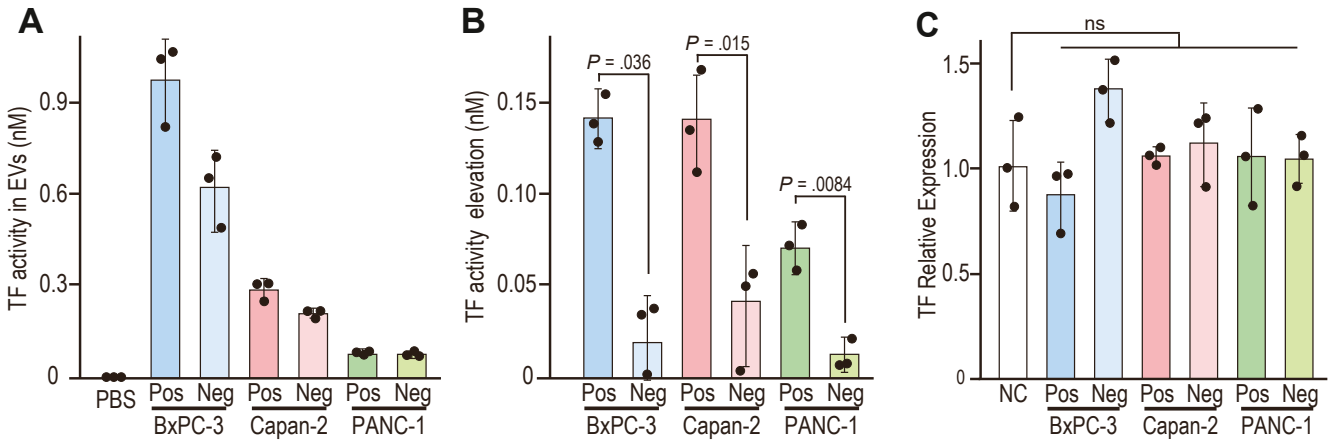

Figure 5. Pancreatic cancer cell-derived EVs have tissue factor (TF) activity. (A) TF activities of the indicated EVs (approximately 3.0×10^{10} particles) were measured. Data mean ± SD ($n = 3$). (B) Increased levels of TF activity from baseline in HUVEC-SELE cells treated with the indicated EVs for 1 h from baseline are shown. Baseline levels of TF activity in HUVEC-SELE cells treated with PBS were used. Increased levels of TF activity in HUVEC-SELE cells were compared after treatment with CA19-9-positive EVs (Pos) and CA19-9-negative EVs (Neg). Data are means ± SD ($n = 3$). *P*-values are shown in figure. (C) TF expression levels in HUVEC-SELE treated with EVs for 1 hour were quantified using RT-qPCR. TF expression levels were compared between cells treated with EVs and those treated with PBS (control). Data are means ± SD ($n = 3$). $P = .41$ (BxPC-3 Pos), $P = .086$ (BxPC-3 Neg), $P = .77$ (Capan-2 Pos), $P = .58$ (Capan-2 Neg), $P = .85$ (PANC-1 Pos), and $P = .89$ (PANC-1 Neg). All statistical analyses were performed using the Welch's *t*-tests. Neg, CA19-9-negative; ns, not significant; Pos, CA19-9-positive.

coagulation factors, TFs were highly expressed in human pancreatic cancer tissues, especially in tissues at advanced stages, which is consistent with a previous report [20] (Figure 4A). Interestingly, TFs were highly expressed in BxPC-3 wild-type cells but hardly expressed in PANC-1 wild-type cells (Figure 4B), suggesting that TF expression was cell type-specific. Consistent with the expression status in the cells, TFs were found in EVs derived from BxPC-3 and Capan-2 cells but were hardly detected in EVs from PANC-1 cells, as determined by western blotting analysis (Figure 4C). Slightly decreased TF levels were observed as different broad bands in EVs derived from FUT3 gene-disrupted BxPC-3 and Capan-2 cells (Figure 4C), which may reflect that disrupting FUT3 also affects the glycosylation levels of TFs and subsequent changes in TF levels; however, the exact reason remains unknown. Although flow cytometry analyses using the beads on which EVs were attached accurately detected the expression of TFs on the surface of EVs derived from BxPC-3 cells and not from PANC-1 cells, the differences could not be detected clearly (Figure 4D). Therefore, we applied the "tag method" to quantitate the TF levels on the surface of EVs. Using this sensitive method, we clearly determined that the expression levels of TFs on the surfaces of EVs derived from BxPC-3 cells were significantly higher than those derived from PANC-1 cells (Figure 4E). Furthermore, we detected TF expression on the surface of EVs isolated from the sera of patients with pancreatic cancer (Figure 4F). Importantly, the results were clearer when CA19-9, which was present on the surface of EVs derived from the serum of cancer patients, was used instead of CD9 as a capture antibody (Figure 4G), probably indicating that analyses using CA19-9 as a capture marker were more tumor-derived EV-specific. This method enabled us to analyze tumor-derived EVs specifically from heterogeneous EV populations in the sera.

TF Activity on Endothelial Cells Was Elevated After the Treatment With CA19-9-Positive EVs

While TFs, determined by the activation levels of the coagulation cascade, could be detected in pancreatic cancer cell line-derived EVs, consistent with previous reports [6–8] (Figure 5A), the activity levels varied mostly in proportion to TF expression levels (Figure 4C). Although TF expression in PANC-1 cells and their EVs was barely recognizable (Figure 4B and C), PANC-1 cell-derived EVs showed slight TF activity (Figure 5A).

To determine differences in TF activity in vascular cells exposed to different types of EVs, HUVEC-SELE were treated with CA19-9-negative and CA19-9-positive EVs derived from various pancreatic cancer cell lines. As shown in Figure 5B, HUVEC-SELE treated with CA19-9-positive EVs showed a significant increase in TF activity compared with HUVEC-SELE treated with CA19-9-negative EVs, irrespective of the cell lines used (Figure 5B). This tendency was also observed even when using the EVs derived from PANC-1 cells (Figure 5B). While the TF activities of CA19-9-positive BxPC-3 EVs were much higher than those of other EVs, the increased levels of the TF activities in HUVEC-SELE treated with these EVs were almost similar to those in HUVEC-SELE treated with CA19-9-positive Capan-2 EVs. This may reflect the reduced adherence of BxPC-3 EVs to HUVEC-SELE, as determined by flow cytometry (Figure 3A).

To determine whether the increased TF activity of HUVEC-SELE cells was dependent on increased TF expression induced by EV treatment, RT-qPCR and RNA sequencing were performed. TF expression levels in HUVEC-SELE did not significantly increase upon the addition of EVs (Figure 5C and Figure A3A). In addition, gene ontology analyses showed that the expression levels of genes associated with blood coagulation were not significantly altered by treatment with BxPC-3 CA19-9-positive EVs (Figure A3B). These results suggest that CA19-9-positive EVs were more likely to adhere to HUVEC-SELE, and the TF activities at the surface of endothelial cells were upregulated because of the TFs in the EVs without transcriptional changes in coagulation factors in endothelial cells. These results may underline the mechanisms of clinically increased cancer-associated VTE in patients with pancreatic cancer among CA19-9-positive cases.

Discussion

Because cancer-associated VTE is a crucial complication in patients with cancer owing to its high mortality rate, interventional methods for the prevention and treatment of VTE are urgently required. We showed that higher levels of CA19-9 in EVs derived from pancreatic cancer cells led to a higher risk of VTE because CA19-9-positive EVs, which express coagulation factor TFs on their surfaces, tend to adhere to endothelial cells via glycoprotein and lectin interactions. These results were confirmed using clinical data and in vitro studies.

Our clinical data revealed that high serum CA19-9 levels were independent risk factors for cancer-associated VTE in patients with pancreatic cancer. Higher levels of CA19-9 in the sera are generally recognized as indicators of cancer progression, but the risk of VTE was not associated with tumor stage and in vitro studies, suggesting a higher CA19-9 level as a risk factor for VTE in pancreatic cancer is not simply due to cancer progression. Particularly, CA19-9 on the surface of EVs derived from cancer cells is crucial for the attachment of EVs to activated endothelial cells expressing SELE, leading to local thrombosis via coagulation factors on the EVs.

Another important point in this study is the establishment of a new "tag method" to detect and quantitate the proteins on the surface of EVs. Because EVs are generally too small for analysis using conventional flow cytometry, it is difficult to quantify the protein of interest on the surface of EVs.[21] Recent progress in single-cell analysis using barcode tags has led to the application of such tag methods in the study of EVs.[22] However, this analysis requires the specific equipment for single-cell analysis, and all researchers cannot perform this analysis. Therefore, in this study, we applied specific oligonucleotide-conjugated antibodies and quantitated the proteins of interest on the surface of EVs by recovering the tags followed by qPCR instead of the direct quantitation of proteins.

While we primarily used antibodies against CD63, which many EVs express on the surface,[4] as a capture antibody to attach the EVs to the microbeads, different capture antibodies can be used according to the experimental objectives. Indeed, when an anti-CA19-9 antibody was used as a capture antibody to hold EVs on the beads, cancer-specific EVs, which were assumed to be derived from cancer cells, could be captured,[11] and TFs on those EVs could be quantitated from the heterogeneous EV population in patient sera. This is another advantage of this method for isolating and characterizing EV subpopulations from a heterogeneous EV population.

Although our results provide new insights into the pathogenesis of cancer-associated VTE in patients with pancreatic cancer, some aspects require further clarification. First, the actual thrombosis formation induced by CA19-9-positive EVs was not determined here, mainly because of the lack of convenient experimental methods to study thrombosis formation without the use of special devices or reagents,[23] whereas the upregulated TF activities of HUVEC-SELE were confirmed after treatment with CA19-9-positive EVs. Second, it cannot be denied that factors other than TFs on the surface of EVs are also involved in cancer-associated VTE.[6] Because TF is not always equally expressed in all pancreatic cancer cells and factors other than CA19-9 may also be involved in the adherence of EVs to endothelial cells, as shown in our analyses using cell lines, the mechanism of individual differences may require further studies. Nonetheless, our results showed that higher levels of CA19-9 in the sera and EVs are risk factors for cancer-associated VTE in patients with pancreatic cancer.

Conclusion

CA19-9 on EVs binds to activated endothelial cells, and increased TF levels and activities locally may cause thrombosis. Considering these results, interventions against CA19-9-positive EVs, such as elimination or neutralization, may be novel therapeutic strategies against cancer-associated VTE in patients with pancreatic cancer.

Supplementary Materials

Material associated with this article can be found in the online version at https://doi.org/10.1016/j.gastha.2024.02.005.

References

1. Khorana AA, Francis CW, Culakova E, et al. Frequency, risk factors, and trends for venous thromboembolism among hospitalized cancer patients. Cancer 2007;110:2339–2346.
2. Khorana AA. Venous thromboembolism and prognosis in cancer. Thromb Res 2010;125:490–493.
3. Mukai M, Oka T. Mechanism and management of cancer-associated thrombosis. J Cardiol 2018;72:89–93.
4. Hallal S, Tűzesi Á, Grau GE, et al. Understanding the extracellular vesicle surface for clinical molecular biology. J Extracell Vesicles 2022;11:e12260.

5. Noubouossie DF, Reeves BN, Strahl BD, et al. Neutrophils: back in the thrombosis spotlight. Blood 2019;133:2186–2197.
6. Abdol Razak NB, Jones G, Bhandari M, et al. Cancer-associated thrombosis: an overview of mechanisms, risk factors, and treatment. Cancers (Basel) 2018;10:380.
7. Che SPY, Park JY, Stokol T. Tissue factor-expressing tumor-derived extracellular vesicles activate quiescent endothelial cells. Front Oncol 2017;7:261.
8. Lima LG, Leal AC, Vargas G, et al. Intercellular transfer of tissue factor via the uptake of tumor-derived microvesicles. Thromb Res 2013;132:450–456.
9. Wang T, Matsuda Y, Nonaka K, et al. Clinicopathological characteristics of gastric cancer with carbohydrate antigen 19-9 expression occurring in elderly individuals: an autopsy study. Pathol Int 2020;70:92–100.
10. Mattila N, Hisada Y, Przybyla B, et al. Levels of the cancer biomarker CA 19-9 are associated with thrombin generation in plasma from treatment-naïve pancreatic cancer patients. Thromb Res 2021;199:21–31.
11. Shibata C, Otsuka M, Seimiya T, et al. Lipolysis by pancreatic cancer-derived extracellular vesicles in cancer-associated cachexia via specific integrins. Clin Transl Med 2022;12:e1089.
12. Engle DD, Tiriac H, Rivera KD, et al. The glycan CA19-9 promotes pancreatitis and pancreatic cancer in mice. Science 2019;364:1156.
13. Edelstein LC, Pan A, Collins T. Chromatin modification and the endothelial-specific activation of the E-selectin gene. J Biol Chem 2005;280:11192–11202.
14. Yoshikawa T, Wu J, Otsuka M, et al. Repression of MicroRNA function mediates inflammation-associated colon tumorigenesis. Gastroenterology 2017;152:631–643.
15. Trinchera M, Aronica A, Dall'Olio F. Selectin ligands sialyl-Lewis a and sialyl-Lewis x in gastrointestinal cancers. Biology (Basel) 2017;6:16.
16. Borosch S, Dahmen E, Beckers C, et al. Characterization of extracellular vesicles derived from cardiac cells in an in vitro model of preconditioning. J Extracell Vesicles 2017;6:1390391.
17. Arab T, Mallick ER, Huang Y, et al. Characterization of extracellular vesicles and synthetic nanoparticles with four orthogonal single-particle analysis platforms. J Extracell Vesicles 2021;10:e12079.
18. Egberts JH, Cloosters V, Noack A, et al. Anti-tumor necrosis factor therapy inhibits pancreatic tumor growth and metastasis. Cancer Res 2008;68:1443–1450.
19. Takaku Y, Suzuki H, Ohta I, et al. A thin polymer membrane, nano-suit, enhancing survival across the continuum between air and high vacuum. Proc Natl Acad Sci U S A 2013;110:7631–7635.
20. Nielsen CH, Jeppesen TE, Kristensen LK, et al. PET imaging of tissue factor in pancreatic cancer using 64Cu-labeled active site-inhibited factor VII. J Nucl Med 2016;57:1112–1119.
21. Liu H, Tian Y, Xue C, et al. Analysis of extracellular vesicle DNA at the single-vesicle level by nano-flow cytometry. J Extracell Vesicles 2022;11:e12206.
22. Stoeckius M, Hafemeister C, Stephenson W, et al. Simultaneous epitope and transcriptome measurement in single cells. Nat Methods 2017;14:865–868.
23. Mangin PH, Neeves KB, Lam WA, et al. In vitro flow-based assay: from simple toward more sophisticated models for mimicking hemostasis and thrombosis. J Thromb Haemost 2021;19:582–587.

Received April 20, 2023. Accepted February 21, 2024.

Correspondence:
Address correspondence to: Motoyuki Otsuka, MD, Department of Gastroenterology, Graduate School of Medicine, The University of Tokyo, 7-3-1 Hongo, Bunkyo-ku, Tokyo 113-8655, Japan. e-mail: otsukamo-tky@umin.ac.jp.

Authors' Contributions:
Chikako Shibata and Motoyuki Otsuka planned and designed the study. Chikako Shibata, Takahiro Seimiya, and Takahiro Kishikawa performed the experiments. Kazunaga Ishigaki acquired the clinical data. Chikako Shibata, Motoyuki Otsuka, and Mitsuhiro Fujishiro analyzed the data and wrote the manuscript.

Conflicts of Interest:
The authors disclose no conflicts.

Funding:
This work was supported by grants-in-aid from the Ministry of Education, Culture, Sports, Science, and Technology, Japan (#20J20625, #22H02828, #22K15958, and #21H02893 to C.S., M.O., T.S., and T.K., respectively), and grants from the Japan Agency for Medical Research and Development (AMED; JP22ck0106557 to M.O.) and JST CREST (#JPMJCR19H5 to M.O.).

Ethical Statement:
The study protocol was approved by the Ethics Committee of the University of Tokyo Hospital (No. 11712).

Data Transparency Statement:
All data, materials, and protocols used in this study are available from the corresponding author on reasonable request.

Reporting Guidelines:
Helsinki Declaration.